Bioorganic Chemistry 83 (2019) 450–460

Contents lists available at ScienceDirect

Bioorganic Chemistry

journal homepage: www.elsevier.com/locate/bioorg

Novel dauricine derivatives suppress cancer via autophagy-dependent cell death

Xiaobo Zhou[1], Yuan Qing Qu[1], Zhiyuan Zheng, Betty Yuen Kwan Law, Simon Wing Fai Mok, Zhi-Hong Jiang*, Vincent Kam Wai Wong*, Li-Ping Bai*

State Key Laboratory of Quality Research in Chinese Medicine, and Macau Institute for Applied Research in Medicine and Health, Macau University of Science and Technology, Taipa, Macau

ARTICLE INFO

Keywords:
Bisbenzylisoquinoline alkaloids
Dauricine derivatives
Carbamate
Autophagy activator
Anti-cancer

ABSTRACT

Eleven dauricine derivatives were synthesized and evaluated for their anti-cancer effect in different cancer cells and their autophagic activity in HeLa model cell. Among these newly synthesized compounds, carbamates **2a**, **2b**, carbonyl ester **3a** and sulfonyl ester **4a** exhibited potent cytotoxic effects on tested cancer cells with IC_{50} values ranged from 2.72 to 12.53 μM, which were more potent than that of dauricine (higher than 15.53 μM). The above four derivatives are validated to induce autophagy-dependent cell death in HeLa cancer cells. These findings offer us a promising source for generating novel autophagic enhancers for anti-cancer therapy.

1. Introduction

Autophagy is a unique recycling mechanism characterized by the formation of double membrane vesicles, which engulf and degrade cytoplasmic materials or damaged organelles via lysosomes degradation, thereby, maintain normal cellular homeostasis of cells [1]. Owing to the crucial role of autophagy in cellular differentiation, development, homeostasis, starvation, and stressful conditions, defect in autophagy induction would contribute to the various diseases including neurodegenerative diseases, infectious diseases, metabolic diseases, and cancers [2]. During cancers therapies, autophagy can act as either a tumor suppressor by the removal of unfolded proteins and damaged organelles, or as a pro-survival mechanism to facilitate the tumor progression and development [3]. Nevertheless, emerging evidence have demonstrated that polyphenolic natural compounds quercetin, genistein, rottlerin, resveratrol [4] and guttiferone K [5] are capable of regulating cancers via the autophagic cell death mechanism [6,7]. Therefore, compounds that can enhance autophagic cell death in cancer cells are highly demanded for anti-cancer therapy.

Dauricine is a bioactive bisbenzylisoquinoline alkaloid isolated from the root of *Menispermum dauricum* D.C. (“Bei-Dou-Gen” in Chinese) commonly used for the treatment of cardiac arrhythmia and inflammatory diseases in clinic [8–10]. Diverse pharmacological activities of dauricine were also reported including protection of cerebral injury [11], induction of cell apoptosis, suppression of cancer cell growth and angiogenesis [12,13]. Our previous findings have identified dauricine and its several analogues as autophagy activators which stimulate autophagic cell death in a panel of apoptosis-resistant cells via AMPK activation [14–16]. Just recently, we further reported that the derivative of dauricine, *N*-desmethyldauricine, activate autophagic cell death in Bax-Bak deficient apoptosis-defective colon cancer cells via Ca^{2+} mobilization [17]. In order to develop more potent autophagy activators, structural modifications were designed and conducted on dauricine by means of carbamation, esterification and sulfonation reactions. Herein, we reported the chemical syntheses of eleven dauricine derivatives and identification of novel activators of autophagy from the newly synthesized dauricine derivatives. It was found that all structurally modified alkaloid compounds in this study could be a novel autophagy activator. Among these compounds, **2a**, **2b**, **3a** and **4a** derivatives were validated to induce autophagic cell death in HeLa cancer cells. Collectively, our work provides novel insight into the autophagic effects of structurally modified alkaloid compounds and their potential uses in anti-cancer treatment.

2. Results and discussion

2.1. Chemistry

The carbamate moiety is a key functionality in many prodrugs and FDA approved drugs [18]. This amide-ester hybrid generally displays

* Corresponding authors.
E-mail addresses: zhjiang@must.edu.mo (Z.-H. Jiang), kawwong@must.edu.mo (V.K.W. Wong), lpbai@must.edu.mo (L.-P. Bai).
[1] These authors contributed equally to this work.

https://doi.org/10.1016/j.bioorg.2018.10.074
Received 31 August 2018; Received in revised form 26 October 2018; Accepted 31 October 2018
Available online 02 November 2018

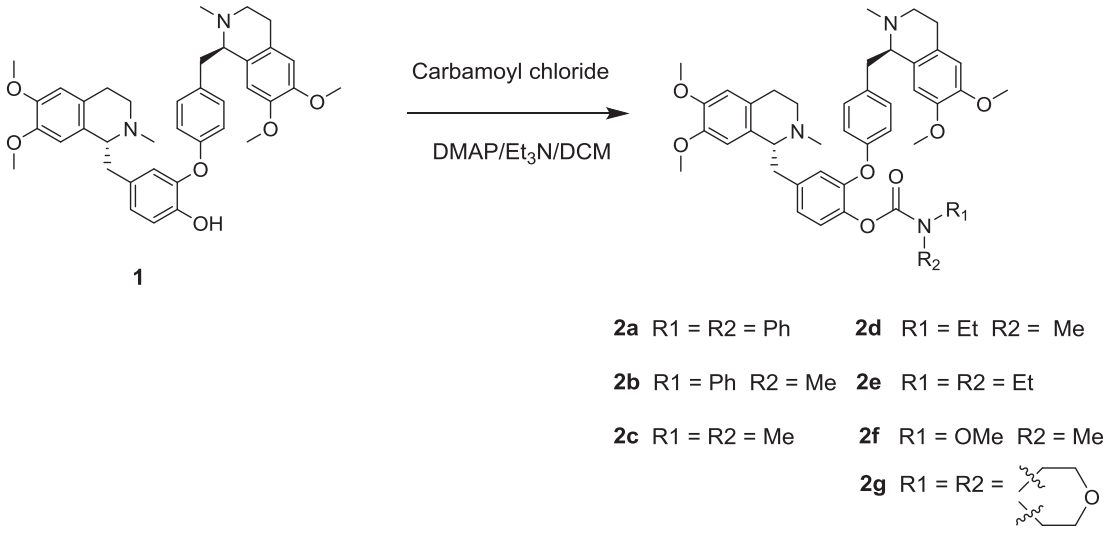

Scheme 1. Syntheses of carbamate derivatives of dauricine (**2a–2g**).

very good chemical and proteolytic stability and may increase permeability across cellular membranes [18]. The carbamate group in *WYE-354*, an ATP-competitive mTOR inhibitor, has been regarded as a necessary motif to increase the autophagy inducing activity in cancer cells [19–20]. Therefore, carbamate substituted dauricine derivatives were designed and successfully synthesized as presented in Scheme 1. Briefly, dauricine reacted with commercially available carbamoyl chlorides at 0 ^{0}C in CH_2Cl_2 in the presence of Et_3N to give seven carbamate derivatives (**2a–2g**). Phenyl and alkyl chains such as methyl, ethyl, methoxyl or morpholinyl groups were introduced into dauricine to evaluate the role of different substituents on the *N*-termini of carbamates. Although it was reported that the presence of barrier to rotation of the C—N bond in carbamate could give rise to two possible *anti* and *syn* stereoisomers, the *syn/anti* equilibrium was often strongly biased on one side [21,22]. Herein, doubling signals of *syn* and *anti* rotamers of were observed in the ^{13}C NMR spectrum of only compound **2d**.

Similarly, ester and sulfonate derivatives of dauricine were also prepared as illustrated in Scheme 2 in order to compare the effects of different linking groups on autophagy activity. Dauricine was treated with Et_3N at 0 ^{0}C in CH_2Cl_2, either carbonyl chloride or sulfonyl chloride was added dropwise at 0 ^{0}C. Then the solution was allowed to room temperature for overnight to afford aromatic carboxylic esters (**3a–3b**), aromatic sulfonic ester (**4a**) and methyl sulfonic ester (**4b**).

2.2. Biological evaluation

2.2.1. Dauricine derivatives induce cytotoxicity and autophagy in cancer cells

Our previous studies demonstrated that dauricine is a direct AMPK activator, it activates autophagy and autophagic cell death in HeLa cancer cells via AMPK-mTOR signaling pathways [14,15]. In contrast, recent study reported that dauricine could act as autophagy blocker and sensitize cancer cells to camptothecin-induced toxicity [23]. Nevertheless, the derivative of dauricine, *N*-desmethyldauricine, was identified as autophagy inducer, it targets sarcoplasmic reticulum Ca^{2+} ATPase (SERCA) for calcium mobilization and thereby induces autophagic cell death in apoptosis-defective cancer [17]. Accordingly, it is interesting to investigate whether the newly synthesized 11 derivatives of dauricine exhibit anti-cancer effect via autophagy induction. Here, we compared the cytotoxicity of dauricine, *N*-desmethyldauricine, and all synthesized 11 derivatives of dauricine (**2a–4b)** in HeLa, A549, HCT-8, Hep-G2, and Du-145 cancer cells. Results showed that dauricine and *N*-desmethyldauricine exhibited potent anti-cancer effect with IC_{50} higher than 15 μM, whereas some of the derivatives of dauricine indicated stronger cytotoxic effect, such as **2a** (mean IC_{50} ranged from 2.72 to 6.25 μM), **2b** (mean IC_{50} ranged from 4.02 to 11.83 μM), **3a** (mean IC_{50} ranged from 3.54 to 11.24 μM) and **4a** (mean IC_{50} ranged from 4.94 to 12.53 μM), the other derivatives of dauricine are less toxic (> 20 μM) compared to their parental compound (Table 1). The toxicities of these four derivatives were further evaluated in normal LO2 (liver) and BEAS-2B (lung) cell lines of human origin. All these four derivatives show low toxicity against LO2 cells with IC_{50} values ranged from 11.58 to 27.15 μM. Derivatives **2b** and **3a** exhibit low cytotoxicity to BEAS-2B cells (Table S1). These findings suggested that the structural modifications of dauricine produce potent anti-cancer compounds.

Supplementary data associated with this article can be found, in the online version, at https://doi.org/10.1016/j.bioorg.2018.10.074.

Autophagy induction contributes to autophagic cell death in some

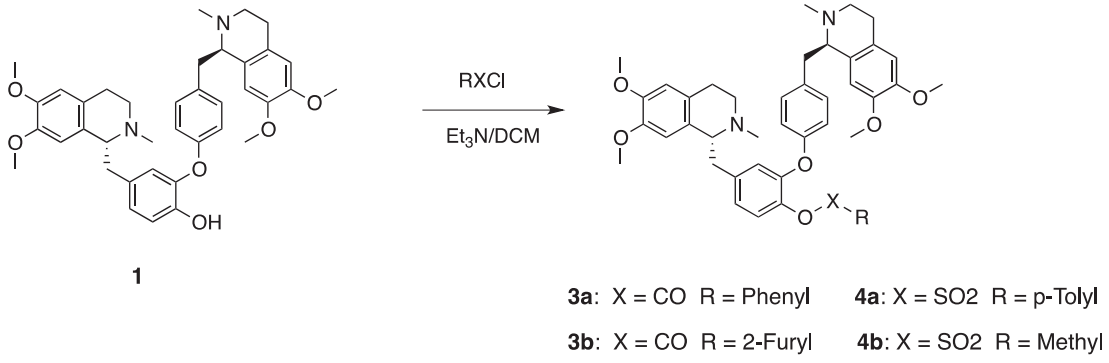

Scheme 2. Syntheses of carboxylate (**3a** and **3b**) and sulfonate (**4a** and **4b**) derivatives of dauricine.

Table 1
Dauricine derivatives induce cytotoxicity in different cancer cells.

IC_{50} Values [μM][a]	Cancer Cells HeLa (Cervical)	A549 (Lung)	HCT-8 (Colon)	Hep G2 (Liver)	Du-145 (Prostate)
Dau	15.53 ± 0.93	> 20	> 20	18.94 ± 1.14	> 20
NDau	15.80 ± 0.47	> 20	> 20	17.45 ± 0.76	> 20
2a	5.44 ± 0.34	6.25 ± 0.61	2.72 ± 0.59	3.04 ± 0.28	3.04 ± 0.44
2b	6.72 ± 0.85	7.16 ± 0.97	11.83 ± 0.39	4.63 ± 0.63	4.02 ± 0.92
2c	> 20	> 20	> 20	> 20	> 20
2d	> 20	> 20	> 20	11.1 ± 0.73	> 20
2e	18.94 ± 2.52	> 20	14.51 ± 1.43	6.13 ± 0.42	> 20
2f	> 20	> 20	> 20	> 20	> 20
2g	> 20	> 20	> 20	12.6 ± 1.17	> 20
3a	6.44 ± 0.60	7.19 ± 0.73	9.05 ± 1.54	3.54 ± 0.38	11.24 ± 0.69
3b	> 20	> 20	> 20	> 20	> 20
4a	6.01 ± 0.08	8.02 ± 0.85	12.53 ± 1.51	4.94 ± 0.68	10.68 ± 0.49
4b	> 20	> 20	> 20	12.7 ± 0.42	> 20

[a] Cancer cells in 96 well-plates were treated with 0 to 20 μM of dauricine (Dau), N- desmethyldauricine (NDau), and dauricine derivatives (**2a–4b**) for 72 h. Cell cytotoxicity was then assessed using the 3-(4, 5-dimethylthiazol-2-yl)-2, 5- diphenyltetrazolium bromide (MTT) (5.0 mg/ml) assay. The IC_{50} values shown in the table are mean values ± S.D. of three independent experiments.

apoptosis-resistant cancers through the inhibition of anti-autophagic proteins [24], thus, identification of novel autophagy enhancers may act as an effective strategy for the discovery of anti-cancer compounds [25]. To evaluate the autophagic effect of dauricine derivatives, the conversion of cytosolic LC3-I to membrane-bound LC3-II, an essential step for the induction of autophagy, was monitored in GFP-LC3 stable expressing HeLa cancer cells [26,27]. As revealed by the increased formation of GFP-LC3 puncta in HeLa cells, untreated control cells indicated no green fluorescence puncta formation, whereas dauricine, *N*-desmethyldauricine and the dauricine derivatives dose-dependently induced autophagic puncta in HeLa cells (Fig. 1). We further determined the presence of the autophagy marker protein, LC3-II [28] in response to the compounds treatment. As shown in Fig. 2 and Supplementary Fig. S1, similar to dauricine and *N*-desmethyldauricine, the derivatives of dauricine dose-dependently increased the conversion of LC3-I to LC3-II indicating the upregulation of autophagosome formation. Taken together, our findings confirmed that the newly synthesized dauricine derivatives could induce autophagy in HeLa cancer cells.

2.2.2. Dauricine derivatives induce cytotoxic autophagic cell death in HeLa cancer cells

To investigate whether the dauricine derivatives-induced autophagy contributes to cell death or acts as pro-survival mechanism [29]. We selected the most potent dauricine derivatives **2a**, **2b**, **3a** and **4a** for MTT assay and Annexin V cell death analysis. As shown in Fig. 3 dauricine derivatives illustrated lower cytotoxicity in Atg7-deficient MEF cells with ablated autophagic response. Such observation indicated that the tested dauricine derivatives are capable of inducing autophagy process and cytotoxic effects to our cancer cell models. Furthermore, Annexin V flow cytometry analysis illustrated that DMSO treatment control and wortmannin (WM), autophagy inhibitor [28] alone exhibited no cytotoxic effect in HeLa cancer cells, whereas the examined dauricine derivatives markedly increase the percentage of cell death upon drug treatment (Fig. 4). Obviously, blocking of autophagy by wortmannin or ablation of Atg7 significantly inhibited these derivatives-mediated cell death. These findings implicated that dauricine derivatives (**2a**, **2b**, **3a** and **4a**)-induced autophagy ultimately led to autophagy-dependent cell death, suggesting the potential development of these novel compounds as anti-cancer agents.

3. Discussion

Our laboratory has previously validated the natural alkaloid small-molecule dauricine can act as autophagy activator and be used therapeutically for cancer treatment. Dauricine is capable of triggering significant cytotoxicity *in vitro* towards cancers of liver, cervix, and lung via the induction of autophagic cell death [14]. In another recently published research work, we further demonstrated that *N*-desmethyldauricine, a derivative of dauricine can increase calcium mobilization, and eventually lead to autophagic cell death in apoptosis-resistant cancer [17]. Such findings tempted us to investigate the effects of structural modification of dauricine with differential types of chemical side chains. Generally, all of the modified dauricine derivatives were toxic to our cellular model with the cytotoxic effects associated with autophagy activation. HeLa cells were specifically chosen for the study since the flattened shape and discrete cellular compartments of these cells provide morphological advantages for observing autophagosome formation. Of note, compounds **2a**, **2b**, **3a** and **4a** demonstrated the most potent cytotoxic effect on HeLa cancer cells among all dauricine derivatives. These four dauricine derivatives showed very close IC_{50} values around 6 μM on HeLa cancer cells, which were at least 2.3-folds increment of activity compared to that of the parent dauricine (15.53 μM). A calculated log *P* (cLog *P*) is routinely used as an assessment of compounds' lipophilicity, which reflects the key event of molecular desolvation in transfer from aqueous phases to cell membranes and to protein binding sites [30]. Table S1 showed that cLog *P* values of selected dauricine derivatives follows the trend of **2a** (9.63) > **3a** (8.58) ~ **4a** (8.54) > **2b** (8.15) > **2e** (7.081) > daurince (6.50). These selected compounds displayed an inverse linear correlation between log IC_{50} and cLog *P* values (r^2 = 0.8250), suggesting that lipophilicity contributes to their cytotoxicity on HeLa cancer cells (Fig. S2). On the other hand, these four compounds (**2a**, **2b**, **3a**, **4a**) are having at least one benzene group (phenyl or tolyl) regardless of the nature of the linkage moieties (carbamate, carboxylic ester or sulfonic ester) in their structures. The resonance movement of electrons within these aromatic rings provides extra stability and may explain the more profound cytotoxic effects of these four compounds towards the tested cancer cells.

4. Conclusions

In conclusion, eleven dauricine derivatives were designed and successfully synthesized including seven carbamates (**2a–2g**), two carbonyl esters (**3a** and **3b**) and two sulfonyl esters (**4a** and **4b**). It was found that all the newly synthesized dauricine derivatives could dose-dependently induce autophagy in HeLa cancer cells. Derivatives **2a**, **2b**, **3a** and **4a** led to cytotoxic autophagy process in HeLa cancer model cells. Among these compounds, carbamates **2a**, **2b**, carbonyl ester **3a** and sulfonyl ester **4a**, which bear at least a benzene ring in their chemical structures, exhibited more potent cytotoxicity than their parental compound dauricine. Our work unraveled an effective method for

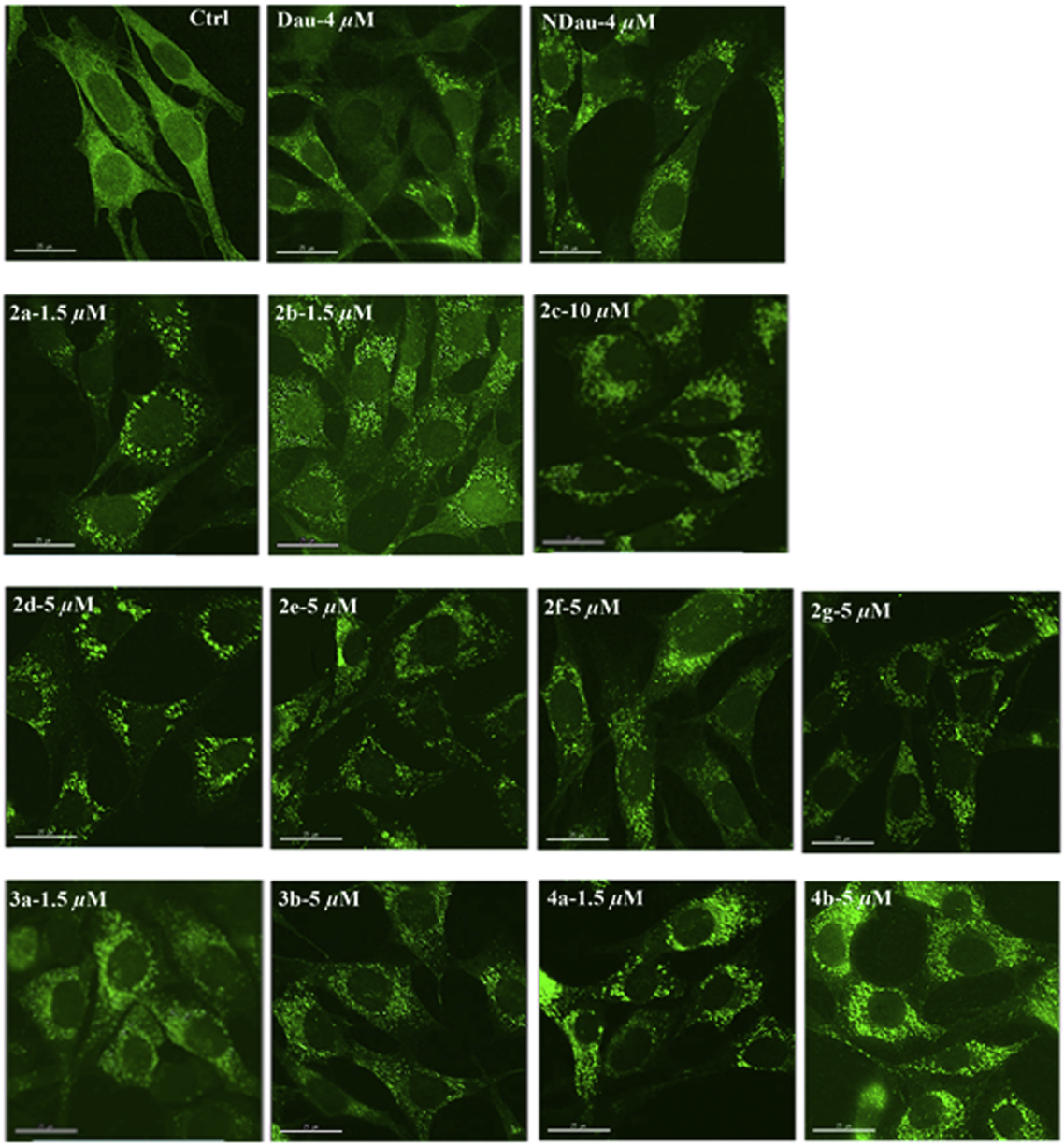

Fig. 1. Identification of dauricine derivatives with autophagic activities. Detection of GFP-LC3 puncta in compound-treated GFP-LC3-HeLa cells. GFP-LC3 stable HeLa cells were treated with DMSO (−ve Ctrl) or the indicated concentrations of dauricine (Dau), *N*-desmethyldauricine (NDau) and dauricine derivatives (**2a**-**4b**) for 24 h. Representative fluorescence images from the highest tested concentration of compound captured at 60X magnification were shown; scale bar, 15 μm. Bar charts represent the quantitation of autophagic cells. The percentages of autophagic cells were calculated as the number of cells with GFP-LC3 puncta (≥10 puncta/cell) divided by the total number of GFP-positive cells in the same field.

producing potent and new autophagic enhancers, which might potentially be developed as anti-cancer agents to treat apoptosis-resistant cancer.

5. Experimental section

5.1. Chemistry

All chemicals and reagents were purchased from Sigma unless otherwise stated. The following regents were used: bafilomycin A1 (Calbiochem, 196000), wortmannin (Santa Cruz, sc-3505), dauricine and *N*-desmethyldauricine (MICXY Reagent, Chengdu, China). We used RIPA lysis buffer (CST, 9806), antibodies against LC3B (CST, 2775) anti-β-actin (Santa Cruz, sc-47778). All the synthesized compounds have a purity of at least 95% determined by UHPLC-UV analysis (Fig. S2). The ^{1}H, ^{13}C NMR experiments were measured on a Bruker Ascend® 600 NMR spectrometer (600 MHz for ^{1}H and 150 MHz for ^{13}C) with the solvent signal as internal reference. High resolution mass spectra (HRMS) were performed on an Agilent 6230 electrospray ionization (ESI) time-of-flight (TOF) mass spectrometer. Melting points are uncorrected and were measured on a MPA100 Optimelt Point Apparatus. Column chromatography was performed with Davisil silica gel (particle size 40–63 μm). Analytical thin layer chromatography (TLC) was performed on Merck silica gel 60-F_{254} plates. Unless otherwise specified, all fine chemicals were used as received. Seven newly designed carbamate compounds were synthesized following the general procedure as belows (see Scheme 1):

An equivalent of appropriate dauricine (20 mg, 0.032 mmol) was dissolved in anhydrous dichloromethane (2 mL), triethylamine (1.5 of equivalents) and appropriate carbamoyl chloride (1.2 of equivalents)

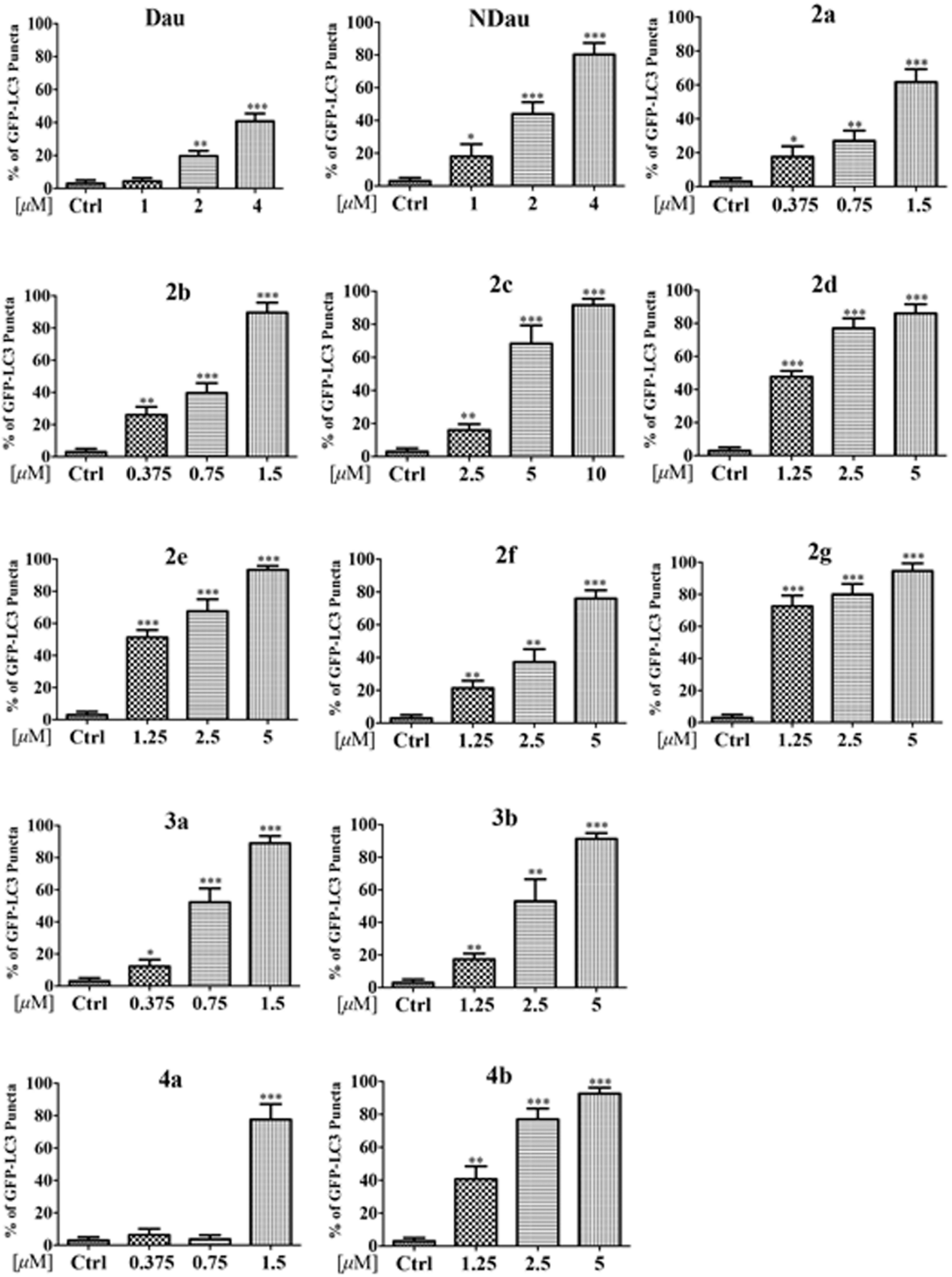

Fig. 1. (*continued*)

were subsequently added, followed by the addition of 4-dimethylaminopyridine (DMAP; 0.1 of equivalents) as a catalyst, and then the mixture was stirred at room temperature for overnight. The reaction was monitored using TLC detection. Finally, the reaction mixture was quenched with water and extracted with dichloromethane. Then, the dichloromethane extract was washed with brine, and further dried over $MgSO_4$. The dichloromethane solvent was evaporated and the residue was purified by chromatography on silica gel to give light yellowish solid of dauricine derivatives (**2a–2g**).

2a: Purification by silica gel column chromatography (10:1 $CHCl_3$/MeOH) afforded 20.5 mg (78%) of **2a** as light yellowish solid. TLC R_f = 0.33 (10: $CHCl_3$/MeOH); Mp 105–107 ^{0}C; $[\alpha]_D^{24} = -62.5^\circ$ (c = 0.2, MeOH); ^{1}HNMR (600 MHz, $CDCl_3$): δ 7.28 (s, 1H), 7.25–7.27 (m, 4H), 7.21 (s, 2H), 7.20 (s, 1H), 7.17 (t, J = 7.8 Hz, 2H), 7.07 (d, J = 8.4 Hz, 1H), 7.04 (s, 1H), 7.04 (s, 1H), 6.85 (s, 1H), 6.84 (dd, J = 8.4 Hz, 2.4 Hz, 1H), 6.84 (s, 1H), 6.68 (d, J = 1.8 Hz, 1H), 6.56 (s, 1H), 6.50 (s,

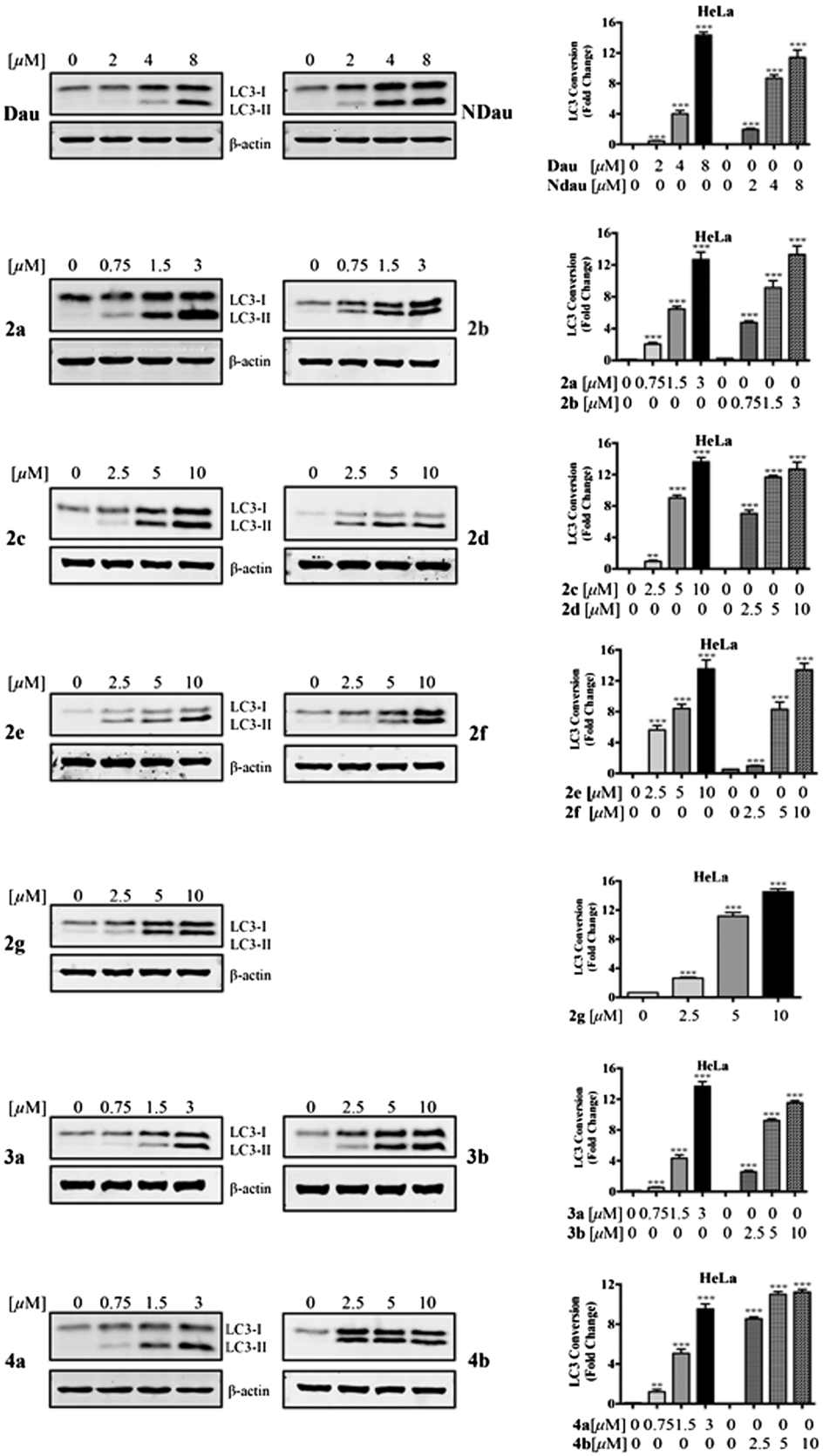

Fig. 2. Dauricine derivatives induce autophagic marker LC3-II conversion. HeLa cancer cells were treated with dauricine (Dau) or its derivatives with three indicated concentrations for 24 h. Cell lysates were analysed by Western blot for LC3 conversion (LC3-I, 18 kDa; LC3-II, 16 kDa) and *β*-actin. LC3-II band intensities were quantified using densitometric analysis and normalised to β-actin. Data are expressed as a fold change relative to the DMSO-treated negative control. Bars are representatives of three independent experiments. Error bars, SEM. *, $P < 0.05$; **, $P < 0.01$; ***, $P < 0.001$.

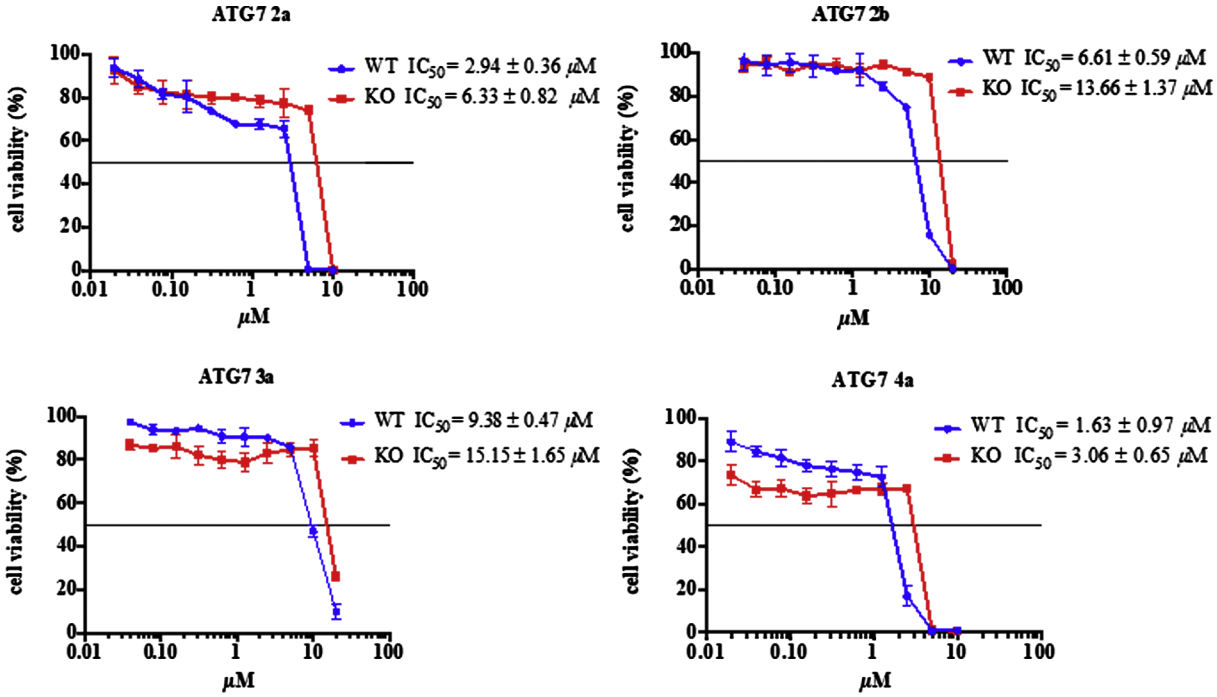

Fig. 3. Dauricine derivatives induce cytotoxic autophagy. Wild type and Atg7-deficient MEF cells were treated with same concentration of dauricine derivatives **2a**, **2b**, **3a** and **4a**. The IC_{50} values were determined by MTT assay. Data represented mean values ± S.D. of three independent experiments.

1H), 6.11 (s, 1H), 6.07 (s, 1H), 3.82 (s, 3H), 3.80 (s, 3H), 3.70 (t, J = 6.0 Hz, 1H), 3.63 (t, J = 6.0 Hz, 1H), 3.61 (s, 3H), 3.54 (s, 3H), 3.15–3.23 (m, 2H), 3.04–3.11 (m, 2H), 2.73–2.84 (m, 5H), 2.56–2.61 (m, 2H), 2.50–2.55 (m, 1H), 2.52 (s, 3H), 2.46 (s, 3H). ^{13}C NMR (150 MHz, $CDCl_3$): δ 155.5, 152.6, 147.8, 147.3, 147.2, 146.4, 146.4, 142.3, 140.6, 138.7, 134.7, 130.8, 128.8, 128.7, 126.2, 126.0, 125.8, 125.1, 123.2, 121.6, 117.7, 111.2, 111.1, 110.9, 110.7, 64.8, 64.5, 55.7, 55.6, 55.5, 46.9, 46.7, 42.6, 42.6, 40.7, 40.5, 25.5, 25.1. HRMS (ESI): m/z for $C_{51}H_{53}N_3O_7$ calcd 819.3884, found 820.3981 $[M+H]^+$, found 410.7049 $[M+2H]^{2+}$.

2b: Purification by silica gel column chromatography (10:1 $CHCl_3$/MeOH) afforded 21.3 mg (88%) of **2b** as light yellowish solid. TLC R_f = 0.33 (10:1 $CHCl_3$/MeOH); Mp 93–95 ^{0}C; $[\alpha]_D^{24} = -90.0^\circ$ (c = 0.2, MeOH); ^{1}HNMR (600 MHz, $CDCl_3$): δ 7.25–7.28 (m, 2H), 7.15–7.20 (m, 3H), 7.05 (s, 1H), 7.04 (d, J = 8.4 Hz, 1H), 7.04 (s, 1H), 6.85 (br, 1H), 6.84 (s, 1H), 6.82 (s, 1H), 6.72 (br, 1H), 6.56 (s, 1H), 6.51 (s, 1H), 6.13 (s, 1H), 6.08 (s, 1H), 3.82 (s, 3H), 3.80 (s, 3H), 3.69 (t, J = 6.0 Hz, 1H), 3.64 (t, J = 6.0 Hz, 1H), 3.63 (s, 3H), 3.58 (s, 3H), 3.18–3.22 (m, 1H), 3.12–3.16 (m, 1H), 3.05–3.11 (m, 2H), 2.81–2.85 (m, 2H), 2.74–2.79 (m, 3H), 2.68–2.72 (m, 1H), 2.54–2.60 (m, 2H), 2.51 (s, 3H), 2.47 (s, 3H). ^{13}C NMR (150 MHz, $CDCl_3$): δ 155.6, 153.3, 147.8, 147.2, 147.2, 146.4, 146.4, 142.9, 140.8, 138.6, 134.5, 130.7, 129.2, 128.8, 128.8, 126.3, 126.0, 125.2, 123.3, 121.8, 111.2, 111.1, 110.9, 110.7, 64.8, 64.5, 55.7, 55.6, 55.5, 46.9, 46.7, 42.6, 42.6, 40.6, 40.5, 38.1, 25.4, 25.2. HRMS (ESI): m/z for $C_{46}H_{51}N_3O_7$ calcd 757.3727, found 758.3826 $[M+H]^+$, 379.6795 $[M+2H]^{2+}$.

2c: Purification by silica gel column chromatography (10:1 $CHCl_3$/MeOH) afforded 20.0 mg (90%) of **2c** as light yellowish solid. TLC R_f = 0.34 (10:1 $CHCl_3$/MeOH); Mp 110–112 ^{0}C; $[\alpha]_D^{24} = -85.7^\circ$ (c = 0.2, MeOH); ^{1}HNMR (600 MHz, $CDCl_3$): δ 7.07 (d, J = 8.4 Hz, 1H), 7.05(s, 1H), 7.04 (s, 1H), 6.88 (dd, J = 8.4 Hz, 2.4 Hz, 1H), 6.84 (s, 1H), 6.83 (s, 1H), 6.77 (d, J = 1.8 Hz, 1H), 6.58 (s, 1H), 6.55 (s, 1H), 6.14 (s, 1H), 6.12 (s, 1H), 3.86 (s, 3H), 3.84 (s, 3H), 3.69–3.73 (m, 2H), 3.68 (s, 3H), 3.63 (s, 3H), 3.20–3.25 (m, 1H), 3.14–3.18 (m, 3H), 2.93 (s, 3H), 2.86 (s, 3H), 2.83–2.87 (m, 1H), 2.75–2.82 (m, 5H), 2.56–2.63 (m, 2H), 2.53 (s, 3H), 2.51 (s, 3H). ^{13}C NMR (150 MHz, $CDCl_3$): δ 155.9, 154.3, 147.9, 147.4, 147.3, 146.5, 146.5, 141.1, 138.4, 134.3, 130.7, 129.1, 128.8, 125.9, 125.4, 123.6, 122.1, 117.4, 111.2, 111.0, 110.8, 64.8, 64.6, 55.8, 55.7, 55.6, 46.9, 46.8, 42.6, 42.6, 40.7, 40.6, 36.8, 36.3, 25.4, 25.2. HRMS (ESI): m/z for $C_{41}H_{49}N_3O_7$ calcd 695.3571, found 696.3602 $[M+H]^+$, 348.6742 $[M+2H]^{2+}$.

2d: Purification by silica gel column chromatography (10:1 $CHCl_3$/MeOH) afforded 20.9 mg (92%) of **2d** as light yellowish solid. TLC R_f = 0.34 (10:1 $CHCl_3$/MeOH); Mp 85–87 ^{0}C; $[\alpha]_D^{24} = -108.0^\circ$ (c = 0.2, MeOH). The *syn* and *anti* rotamers' doubling signals were observed in ^{13}C NMR due to the barrier of *N*-CO rotation in carbamate moiety. ^{1}HNMR (600 MHz, $CDCl_3$): δ 7.10 (d, J = 8.4 Hz, 1H), 7.05(s, 1H), 7.03 (s, 1H), 6.88 (dd, J = 8.4 Hz, 2.4 Hz, 1H), 6.84 (s, 1H), 6.83 (s, 1H), 6.77 (d, J = 1.8 Hz, 1H), 6.57 (s, 1H), 6.54 (s, 1H), 6.15 (s, 1H), 6.15 (s, 1H), 3.86 (s, 3H), 3.84 (s, 3H), 3.69–3.73 (m, 2H), 3.67 (s, 3H), 3.63 (s, 3H), 3.28–3.32 (m, 2H), 3.17–3.23 (m, 1H), 3.10–3.15 (m, 3H), 2.81–2.85 (m, 2H), 2.80 (s, 3H), 2.72–2.76 (m, 2H), 2.56–2.62 (m, 2H), 2.53 (s, 3H), 2.50 (s, 3H), 1.08 (t, J = 7.2 Hz, 3H). ^{13}C NMR (150 MHz, $CDCl_3$): δ 156.0 (155.8), 154.1 (153.8), 147.9, 147.8, 147.3, 146.5, 146.5, 141.2 (141.1), 138.4, 134.5 (134.3), 130.7, 129.3 (129.0), 126.0, 125.5 (125.3), 123.6 (123.6), 122.3 (121.9), 117.5 (117.2), 111.2, 111.2, 111.0, 110.8, 64.8, 64.6, 55.8, 55.7, 55.6, 46.9, 46.9 (46.8), 44.1, 44.0, 42.7, 42.7, 40.7, 34.3, 33.6, 25.5, 25.3, 12.9 (12.4). HRMS (ESI): m/z for $C_{42}H_{51}N_3O_7$ calcd 709.3727, found 710.3706 $[M+H]^+$, 355.6884 $[M+2H]^{2+}$.

2e: Purification by silica gel column chromatography (10:1 $CHCl_3$/MeOH) afforded 20.4 mg (88%) of **2e** as light yellowish solid. TLC R_f = 0.34 (10:1 $CHCl_3$/MeOH); Mp 103–105 ^{0}C; $[\alpha]_D^{24} = -81.8^\circ$ (c = 0.2, MeOH); ^{1}HNMR (600 MHz, $CDCl_3$): δ 7.11 (d, J = 8.4 Hz, 1H), 7.04 (s, 1H), 7.03 (s, 1H), 6.88 (dd, J = 8.4 Hz, 2.4 Hz, 1H), 6.84 (s, 1H), 6.83 (s, 1H), 6.74 (d, J = 1.8 Hz, 1H), 6.58 (s, 1H), 6.54 (s, 1H), 6.10 (s, 1H), 6.12 (s, 1H), 3.86 (s, 3H), 3.83 (s, 3H), 3.69–3.72 (m, 2H), 3.67 (s, 6H), 3.61 (s, 3H), 3.30–3.31 (m, 2H), 3.20–3.25 (m, 3H), 3.11–3.18 (m, 3H), 2.83–2.87 (m, 1H), 2.75–2.82 (m, 5H), 2.55–2.62 (m, 2H), 2.54 (s, 3H), 2.51 (s, 3H), 1.09 (t, J = 12.6 Hz, 6H). ^{13}C NMR (150 MHz, $CDCl_3$): δ 155.8, 153.7, 147.9, 147.4, 147.3, 146.5, 146.5, 141.2, 138.1, 134.2, 130.7, 129.0, 128.8, 125.8, 125.8, 125.3, 123.6, 121.9, 117.4, 111.2, 111.0, 110.9, 64.8, 64.6, 55.8, 55.7, 55.6, 46.8, 46.7, 42.6, 42.5, 42.2, 41.9, 40.7, 40.6, 25.4, 25.2, 13.9, 13.3. HRMS

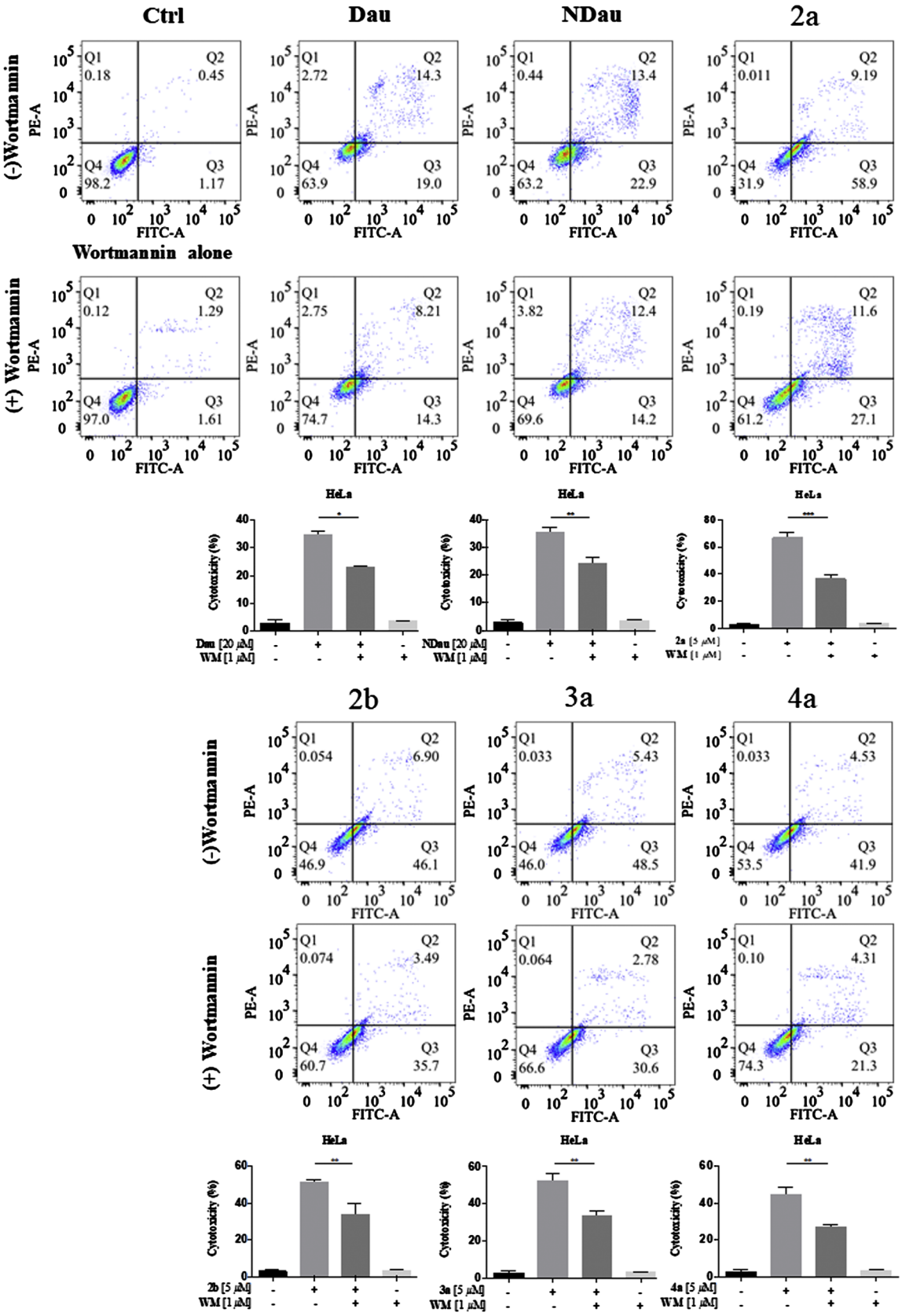

Fig. 4. Dauricine derivatives induce autophagy cell death in HeLa cancer cells. Autophagic inhibitor, wortmannin abrogated the cell death induced by dauricine derivatives **2a**, **2b**, **3a, 4a** and their parental compounds in HeLa cancer cells. HeLa cells treated with dauricine derivatives (5 μM) and parental compounds (20 μM) in the presence or absence of 1 μM of wortmannin for 24 h were assayed by flow cytometry after annexin V staining. Bar charts represent the quantitation of cell death (%).

(ESI): *m/z* for $C_{43}H_{53}N_3O_7$ calcd 723.3884, found 724.4013 $[M+H]^+$, 362.7045 $[M+2H]^{2+}$.

2f: Purification by silica gel column chromatography (10:1 $CHCl_3$/MeOH) afforded 21.2 mg (93%) of **2f** as light yellowish solid. TLC R_f = 0.32 (10:1 $CHCl_3$/MeOH); Mp 84–86 ^{0}C; $[\alpha]_D^{24} = -81.3°$ (c = 0.2, MeOH); ^{1}HNMR (600 MHz, $CDCl_3$): δ 7.12 (d, *J* = 8.4 Hz, 1H), 7.06 (s, 1H), 7.04 (s, 1H), 6.89 (dd, *J* = 8.4 Hz, 2.4 Hz, 1H), 6.86 (s, 1H), 6.84 (s, 1H), 6.73 (d, *J* = 1.8 Hz, 1H), 6.58 (s, 1H), 6.54 (s, 1H), 6.14 (s, 1H), 6.09 (s, 1H), 3.86 (s, 3H), 3.83 (s, 3H), 3.68–3.73 (m, 2H), 3.66 (s, 6H), 3.63 (s, 3H), 3.19–3.22 (m, 1H), 3.18(s, 3H), 3.10–3.17 (m, 3H), 2.83–2.87 (m, 1H), 2.75–2.82 (m, 5H), 2.55–2.62 (m, 2H), 2.53 (s, 3H), 2.51 (s, 3H). ^{13}C NMR (150 MHz, $CDCl_3$): δ 155.5, 154.5, 148.0, 147.3, 146.5, 146.5, 140.4, 138.9, 134.7, 130.9, 130.9, 130.8, 129.1, 128.7, 125.9, 125.3, 123.3, 121.8, 117.8, 117.8, 117.7, 111.2, 111.2, 111.0, 110.8, 64.8, 64.6, 61.5, 55.8, 55.7, 55.6, 46.9, 46.7, 42.6, 42.6, 40.7, 40.6, 35.6, 25.4, 25.2. HRMS (ESI): *m/z* for $C_{41}H_{49}N_3O_8$ calcd 711.3520, found 712.3595 $[M+H]^+$, 356.6852 $[M+2H]^{2+}$.

2 g: Purification by silica gel column chromatography (10:1 $CHCl_3$/MeOH) afforded 22.0 mg (93%) of **2 g** as light yellowish solid. TLC R_f = 0.32 (10:1 $CHCl_3$/MeOH); Mp 104–106 ^{0}C; $[\alpha]_D^{24} = -76.8°$ (c = 0.2, MeOH); ^{1}HNMR (600 MHz, $CDCl_3$): δ 7.10 (d, *J* = 8.4 Hz, 1H), 7.06 (s, 1H), 7.04 (s, 1H), 6.90 (dd, *J* = 8.4 Hz, 2.4 Hz, 1H), 6.83 (s, 1H), 6.81 (s, 1H), 6.80 (d, *J* = 1.8 Hz, 1H), 6.58 (s, 1H), 6.55 (s, 1H), 6.18 (s, 1H), 6.14 (s, 1H), 3.86 (s, 3H), 3.84 (s, 3H), 3.69–3.72 (m, 2H), 3.67 (s, 6H), 3.66 (s, 3H), 3.52 (m, 2H), 3.48 (m, 2H), 3.40 (m, 2H), 3.18–3.21 (m, 1H), 3.10–3.18 (m, 3H), 2.78–2.85 (m, 5H), 2.73–2.78 (m, 1H), 2.57–2.62 (m, 2H), 2.52 (s, 3H), 2.51 (s, 3H), 1.96 (m, 2H). ^{13}C NMR (150 MHz, $CDCl_3$): δ 155.8, 153.1, 147.5, 147.3, 147.3, 146.5, 140.9, 138.7, 134.5, 130.7, 129.2, 128.9, 126.1, 126.0, 125.6, 123.5, 122.3, 117.0, 111.2, 111.2, 111.0, 110.8, 66.6, 66.4, 64.8, 64.6, 55.9, 55.7, 55.7, 46.9, 46.8, 44.9, 44.2, 42.7, 42.6, 40.7, 40.7, 25.5, 25.2. HRMS (ESI): *m/z* for $C_{43}H_{51}N_3O_8$ calcd 737.3676, found 738.3748 $[M+H]^+$, 369.6919 $[M+2H]^{2+}$.

An equivalent of appropriate dauricine (20 mg, 0.032 mmol) was dissolved in dry dichloromethane (2 mL), and triethylamine (1.5 of equivalents) was added in one portion. Either carbonyl chloride or sulfonyl chloride (1.5 of equivalents) was subsequently added, and the mixture was stirred at room temperature for overnight. The reaction was monitored using TLC detection. The reaction mixture was quenched with water and extracted with dichloromethane. The dichloromethane extract was washed with brine, and then dried over $MgSO_4$. Finally, the solvent was evaporated and the residue was purified by column chromatography on silica gel to give light yellowish solid of dauricine derivatives (**3a**, **3b, 4a** and **4b**).

3a: Purification by silica gel column chromatography (10:1 $CHCl_3$/MeOH) afforded 19.1 mg (82%) of **3a** as light yellowish solid. TLC R_f = 0.34 (10:1 $CHCl_3$/MeOH); Mp 103–105 ^{0}C; $[\alpha]_D^{24} = -87.4°$ (c = 0.2, MeOH); ^{1}HNMR (600 MHz, $CDCl_3$): δ 8.09 (dd, *J* = 1.8 Hz, 0.6 Hz, 1H), 8.08 (dd, *J* = 3.6 Hz, 0.6 Hz, 1H), 7.59 (m, 1H), 7.45–7.47 (m, 2H), 7.17 (d, *J* = 8.4 Hz, 1H), 7.01 (s, 1H), 7.00 (s, 1H), 6.94 (dd, *J* = 8.4 Hz, 2.4 Hz, 1H), 6.85 (s, 1H), 6.83 (s, 1H), 6.78 (d, *J* = 1.8 Hz, 1H), 6.56 (dd, *J* = 3.6 Hz, 1.8 Hz, 1H), 6.55 (s, 1H), 6.12 (s, 1H), 5.99 (s, 1H), 3.85 (s, 3H), 3.84 (s, 3H), 3.68–3.74 (m, 2H), 3.70 (s, 3H), 3.46 (s, 3H), 3.19–3.23 (m, 2H), 3.17–3.18 (m, 1H), 3.15–3.16 (m, 1H), 2.83–2.87(m, 2H), 2.75–2.82 (m, 4H), 2.57–2.62 (m, 2H), 2.53 (s, 3H), 2.52 (s, 3H). ^{13}C NMR (150 MHz, $CDCl_3$): δ 164.7, 155.5, 148.2, 147.4, 147.3, 146.5, 146.3, 140.3, 139.1, 134.7, 133.5, 130.8, 130.2, 129.3, 128.9, 128.7, 128.5, 125.9, 125.7, 125.3, 123.2, 121.7, 117.9, 111.2, 111.2, 111.0, 110.8, 64.9, 64.6, 55.8, 55.8, 55.4, 46.8, 46.7, 42.6, 42.5, 40.6, 25.4, 25.2. HRMS (ESI): *m/z* for $C_{45}H_{48}N_2O_7$ calcd 728.3462, found 729.3527 $[M+H]^+$, 365.1800 $[M+2H]^{2+}$.

3b: Purification by silica gel column chromatography (10:1 $CHCl_3$/MeOH) afforded 19.6 mg (85%) of **3b** as light yellowish solid. TLC R_f = 0.33 (95:5 $CHCl_3$/MeOH); Mp 112–114 ^{0}C; $[\alpha]_D^{24} = -97.8°$ (c = 0.2, MeOH); ^{1}HNMR (600 MHz, $CDCl_3$): δ 7.64 (dd, *J* = 1.8 Hz, 0.6 Hz, 1H), 7.27 (dd, *J* = 3.6 Hz, 0.6 Hz, 1H), 7.15 (d, *J* = 7.8 Hz, 1H), 7.03 (s, 1H), 7.02 (s, 1H), 6.91 (dd, *J* = 8.4 Hz, 2.4 Hz, 1H), 6.87 (s, 1H), 6.85 (s, 1H), 6.74 (d, *J* = 1.8 Hz, 1H), 6.57 (s, 1H), 6.55 (dd, *J* = 3.6 Hz, 1.8 Hz, 1H), 6.55 (s, 1H), 6.07 (s, 1H), 6.04 (s, 1H), 3.85 (s, 3H), 3.84 (s, 3H), 3.69–3.72 (m, 2H), 3.68 (s, 3H), 3.53 (s, 3H), 3.18–3.23 (m, 1H), 3.12–3.18 (m, 3H), 2.81–2.88 (m, 2H), 2.74–2.80 (m, 4H), 2.56–2.61 (m, 2H), 2.53 (s, 3H), 2.52 (s, 3H). ^{13}C NMR (150 MHz, $CDCl_3$): δ 156.4, 155.2, 148.4, 147.3, 147.2, 147.9, 146.4, 146.3, 143.7, 139.4, 139.3, 135.0, 130.8, 129.1, 128.7, 125.9, 125.9, 125.1, 123.1, 121.5, 119.4, 118.2, 112.1, 111.2, 111.1, 111.0, 110.8, 64.8, 64.6, 55.8, 55.7, 55.5, 46.8, 46.7, 42.7, 42.6, 40.7, 25.5, 25.3. HRMS (ESI): *m/z* for $C_{43}H_{46}N_2O_8$ calcd 718.3254, found 719.3293 $[M+H]^+$, 360.1557 $[M+2H]^{2+}$.

4a: Purification by silica gel column chromatography (10:1 $CHCl_3$/MeOH) afforded 17.0 mg (74%) of **4a** as light yellowish solid. TLC R_f = 0.32 (10:1 $CHCl_3$/MeOH); Mp 117–119 ^{0}C; $[\alpha]_D^{24} = -53.2°$ (c = 0.2, MeOH); ^{1}HNMR (600 MHz, $CDCl_3$): δ 7.71 (s, 1H), 7.70 (s, 1H), 7.24 (s, 1H), 7.23 (s, 1H), 7.15 (d, *J* = 8.4 Hz, 1H), 6.97 (s, 1H), 6.96 (s, 1H), 6.82 (dd, *J* = 8.4 Hz, 2.4 Hz, 1H), 6.56 (s, 1H), 6.54 (d, *J* = 8.4 Hz, 1H), 6.53 (s, 1H), 6.52 (s, 1H), 6.49 (s, 1H), 6.08 (s, 1H), 6.05 (s, 1H), 3.84 (s, 3H), 3.80 (s, 3H), 3.68–3.70 (m, 1H), 3.63 (s, 3H), 3.62–3.63 (m, 1H), 3.58 (s, 3H), 2.99–3.21 (m, 4H), 2.65–2.80 (m, 6H), 2.55–2.59 (m, 1H), 2.52 (s, 3H), 2.46–2.51 (m, 1H), 2.45 (s, 3H), 2.41 (s, 3H). ^{13}C NMR (150 MHz, $CDCl_3$): δ 154.5, 148.3, 147.3, 147.2, 146.5, 146.3, 145.0, 140.2, 138.3, 134.9, 133.1, 130.7, 129.5, 129.0, 128.6, 128.5, 126.3, 125.9, 124.9, 123.9, 121.3, 117.7, 111.1, 110.9, 110.6, 64.7, 64.3, 55.7, 55.6, 55.6, 47.1, 46.7, 42.6, 42.6, 40.6, 40.5, 25.6, 25.2, 21.6. HRMS (ESI): *m/z* for $C_{45}H_{50}N_2O_8S$ calcd 778.3288, found 779.3325 $[M+H]^+$, 390.1715 $[M+2H]^{2+}$.

4b: Purification by silica gel column chromatography (10:1 $CHCl_3$/MeOH) afforded 20.0 mg (89%) of **4b** as light yellowish solid. TLC R_f = 0.32 (10:1 $CHCl_3$/MeOH); Mp 92–94 ^{0}C; $[\alpha]_D^{24} = -82.7°$ (c = 0.2, MeOH); ^{1}H NMR (600 MHz, $CDCl_3$): δ 7.29 (d, *J* = 8.4 Hz, 1H), 7.08 (s, 1H), 7.07 (s, 1H), 6.94 (dd, *J* = 8.4 Hz, 1.8 Hz, 1H), 6.82 (s, 1H), 6.81 (s, 1H), 6.70 (d, *J* = 2.4 Hz, 1H), 6.58 (s, 1H), 6.53 (s, 1H), 6.13 (s, 1H), 6.08 (s, 1H), 3.86 (s, 3H), 3.83 (s, 3H), 3.67–3.75 (m, 2H), 3.65 (s, 3H), 3.64 (s, 3H), 3.07–3.24 (m, 4H), 3.17 (s, 3H), 2.72–2.88 (m, 6H), 2.58–2.61 (m, 2H), 2.54 (s, 3H), 2.49 (s, 3H). ^{13}C NMR (150 MHz, $CDCl_3$): δ 154.6, 148.0, 147.4, 147.3, 146.5, 146.5, 140.7, 138.5, 135.4, 131.1, 128.4, 126.2, 126.0, 125.5, 124.5, 121.8, 117.7, 111.2, 111.2, 110.9, 110.6, 64.7, 64.4, 55.8, 55.7, 55.7, 55.6, 46.8, 46.7, 42.6, 42.6, 40.6, 40.6, 25.3, 25.2. HRMS (ESI): *m/z* for $C_{39}H_{46}N_2O_8S$ calcd 702.2975, found 703.3045 $[M+H]^+$, 352.1547 $[M+2H]^{2+}$.

5.2. Biological assay

5.2.1. Cell culture

All cells were obtained from the American Type Culture Collection (Rockville, MD, USA) unless otherwise specified. Immortalized Atg7-wild-type and Atg7-deficent mouse embryonic fibroblasts (MEF) were kindly provided by Professor Masaaki Komatsu (Juntendo University, School of Medicine, Japan). GFP-LC3 HeLa stable cells were kindly provided by Professor Li Min (School of Pharmaceutical Sciences, Sun-Yat-Sen University, Guangzhou, China). All media were supplemented with 10% fetal bovine serum and the antibiotics penicillin (50 U/ml) and streptomycin (50 μg/ml; Invitrogen, Paisley, Scotland, UK). All cell cultures were incubated at 37 °C in a 5% humidified CO_2 incubator.

5.2.2. Autophagy LC3 puncta detection

The detection of LC3 autophagic puncta was conducted using GFP-LC3 stable HeLa cancer cells as described below. In brief, compounds-treated GFP-LC3-HeLa cells on cover slips were fixed with 4% paraformaldehyde (Sigma) for 20 min at room temperature and then rinsed with PBS. The coverslips were then mounted with FluorSave™ mounting media (Calbiochem, San Diego, CA, USA) for fluorescence imaging and the localization of LC3 autophagosomes were captured under the API Delta Vision Live-cell Imaging System (Applied Precision Inc., GE

Healthcare Company, Washington, USA). To quantify autophagy, guidelines were followed to monitor autophagy [28], the percentage of cells with punctuate LC3 immunofluorescence staining was calculated by counting the number of the cells showing the increased punctuate pattern of LC3 fluorescence (≥10 dots/cell) in immunofluorescence-positive cells over the total number of cells in the same field. A minimum of 1000 cells from randomly selected fields were scored.

5.2.3. Cytotoxicity assays

All test compounds were dissolved in DMSO at final concentrations of 50 mmol/L and stored at -20°Cbefore use. Cytotoxicity was assessed using the 3-(4, 5-dimethylthiazol-2-yl)-2, 5-diphenyltetrazolium bromide (MTT) (5.0 mg/ml) assay as previously described [31]. Briefly, 4×10^3 cells were seeded per well in 96-well plates before drug treatment. After overnight culture, the cells were then exposed to different concentrations of test compounds (0.039–20 μmol/L) for 72 h. Cells without drug treatment were used as control. Subsequently, MTT (10 μL) was added to each well and incubated at 37 °C for 4 h followed by the addition of 100 μL solubilization buffer (10% SDS in 0.01 mol/L HCl) and overnight incubation. A_{570} nm was determined from each well on the next day. The percentage of cell viability was calculated using the following formula: Cell viability (%) = $A_{treated}/A_{control} \times 100$. Data were obtained from triplication independent experiments.

5.2.4. Annexin V detection by flow cytometry analysis

Apoptosis was detected by Annexin V staining kit (BD Biosciences, San Jose, CA, USA). In brief, cells were exposed to the indicated concentrations of dauricine derivatives for 24 h. Cells were then harvested and analyzed by flow cytometry using FITC-Annexin V and Propidium Iodide staining according to the manufacturer's instructions. Apoptotic cells were quantitatively counted by a flow cytometer (BD FACSAria III, San Jose, CA, USA). Data acquisition and analysis were performed with CellQuest (BD Biosciences, San Jose, CA, USA) from triple independent experiments.

5.2.5. Protein extraction and Western Blotting

After drug treatment, adherent and floating cells were lysed with RIPA lysis buffer. Protein concentrations were determined using the Bio-Rad protein assay (Bio-Rad Laboratories, Inc., Hercules, CA, USA). The cell lysates of samples were subjected to electrophoresis on SDS polyacrylamide gels and transferred to Hybond enhanced chemiluminescence nitrocellulose membranes (Amersham Biosciences, Piscataway, NJ), which were then blocked with 5% non-fat dry milk protein for 1hrs. Membranes were then incubated with the indicated primary antibodies overnight at 4 °C. The binding of the antibody was visualized by peroxidase-coupled secondary antibody using the ECL Western Blotting Detection Reagents (Invitrogen, Paisley, Scotland, UK). Band intensities were quantified by using the software ImageJ (NIH, Bethesda, MD, USA).

5.2.6. Statistical analysis

The results were expressed as means ± S.D. as indicated. The difference was considered statistically significant when the p-value was < 0.05. Student's *t*-test or one-way ANOVA analysis was used for comparison among different groups.

Conflict of interest

The authors confirmed that this article content has no conflict of interest.

Acknowledgements

This work was financially supported by FDCT grants from the Macao Science and Technology Development Fund (015/2017/AFJ to Zhi-Hong Jiang, 056/2013/A2 to Li-Ping Bai and 084/2013/A3 to Vincent Kam Wai Wong). The content is solely the responsibility of the authors. The funders had no role in study design, data collection and analysis, decision to publish, or preparation of the manuscript.

References

[1] B. Levine, G. Kroemer, Autophagy in the pathogenesis of disease, Cell 132 (1) (2008) 27–42.
[2] P.D. Jiang, N. Mizushima, Autophagy and human diseases, Cell Res. 24 (1) (2014) 69–79.
[3] Z.J. Yang, C.E. Chee, S. Huang, F.A. Sinicrope, The role of autophagy in cancer: therapeutic implications, Mol. Cancer Ther. 10 (9) (2011) 1533–1541.
[4] N. Hasima, B. Ozpolat, Regulation of autophagy by polyphenolic compounds as a potential therapeutic strategy for cancer, Cell Death Dis. 5 (2014) e1509.
[5] M. Wu, Y. Lao, N. Xu, X. Wang, H. Tan, W. Fu, Z. Lin, H. Xu, Guttiferone K induces autophagy and sensitizes cancer cells to nutrient stress-induced cell death, Phytomedicine 22 (10) (2015) 902–910.
[6] W. Bursch, A. Ellinger, H. Kienzl, L. Torok, S. Pandey, M. Sikorska, R. Walker, R.S. Hermann, Active cell death induced by the anti-estrogens tamoxifen and ICI 164 384 in human mammary carcinoma cells (MCF-7) in culture: the role of autophagy, Carcinogenesis 17 (8) (1996) 1595–1607.
[7] M.C. Maiuri, E. Zalckvar, A. Kimchi, G. Kroemer, Self-eating and self-killing: crosstalk between autophagy and apoptosis, Nat. Rev. Mol. Cell Bio. 8 (9) (2007) 741–752.
[8] J.Q. Qian, Cardiovascular pharmacological effects of bisbenzylisoquinoline alkaloid derivatives, Acta Pharmacol. Sin. 23 (12) (2002) 1086–1092.
[9] X.Y. Yang, S.Q. Jiang, L. Zhang, Q.N. Liu, P.L. Gong, Inhibitory effect of dauricine on inflammatory process following focal cerebral ischemia/reperfusion in rats, Am. J. Chin. Med. 35 (3) (2007) 477–486.
[10] J. Zhao, Y. Lian, C. Lu, L. Jing, H. Yuan, S. Peng, Inhibitory effects of a bisbenzylisoquinline alkaloid dauricine on HERG potassium channels, J. Ethnopharmacol. 141 (2) (2012) 685–691.
[11] Y.H. Li, P.L. Gong, Neuroprotective effects of dauricine against apoptosis induced by transient focal cerebral ischaemia in rats via a mitochondrial pathway, Clin. Exp. Pharmacol. Physiol. 34 (3) (2007) 177–184.
[12] Z. Yang, C. Li, X. Wang, C. Zhai, Z. Yi, L. Wang, B. Liu, B. Du, H. Wu, X. Guo, M. Liu, D. Li, J. Luo, Dauricine induces apoptosis, inhibits proliferation and invasion through inhibiting NF-kappaB signaling pathway in colon cancer cells, J. Cell Physiol. 225 (1) (2010) 266–275.
[13] J. Wang, Y. Li, X.B. Zu, M.F. Chen, L. Qi, Dauricine can inhibit the activity of proliferation of urinary tract tumor cells, Asian Pac. J. Trop. Med. 5 (12) (2012) 973–976.
[14] B.Y. Law, W.K. Chan, S.W. Xu, J.R. Wang, L.P. Bai, L. Liu, V.K. Wong, Natural small-molecule enhancers of autophagy induce autophagic cell death in apoptosis-defective cells, Sci. Rep. 4 (2014) 5510.
[15] B.Y. Law, S.W. Mok, W.K. Chan, S.W. Xu, A.G. Wu, X.J. Yao, J.R. Wang, L. Liu, V.K. Wong, Hernandezine, a novel AMPK activator induces autophagic cell death in drug-resistant cancers, Oncotarget 7 (7) (2016) 8090–8104.
[16] B.Y.K. Law, F. Gordillo-Martinez, Y.Q. Qu, N. Zhang, S.W. Xu, P.S. Coghi, S.W.F. Mok, J.R. Guo, W. Zhang, E.L.H. Leung, X.X. Fan, A.G. Wu, W.K. Chan, X.J. Yao, J.R. Wang, L. Liu, V.K.W. Wong, Thalidezine, a novel AMPK activator, eliminates apoptosis-resistant cancer cells through energy-mediated autophagic cell death, Oncotarget 8 (18) (2017) 30077–30091.
[17] B.Y.K. Law, S.W.F. Mok, J. Chen, F. Michelangeli, Z.H. Jiang, Y. Han, Y.Q. Qu, A.C.L. Qiu, S.W. Xu, W.W. Xue, X.J. Yao, J.Y. Gao, M.U. Javed, P. Coghi, L. Liu, V.K.W. Wong, N-desmethyldauricine induces autophagic cell death in apoptosis-defective cells via Ca^{2+} Mobilization, Front Pharmacol 8 (2017) 388.
[18] A.K. Ghosh, M. Brindisi, Organic carbamates in drug design and medicinal chemistry, J. Med. Chem. 58 (7) (2015) 2895–2940.
[19] K. Yu, L. Toral-Barza, C. Shi, W.G. Zhang, J. Lucas, B. Shor, J. Kim, J. Verheijen, K. Curran, D.J. Malwitz, D.C. Cole, J. Ellingboe, S. Ayral-Kaloustian, T.S. Mansour, J.J. Gibbons, R.T. Abraham, P. Nowak, A. Zask, Biochemical, cellular, and in vivo activity of novel ATP-competitive and selective inhibitors of the mammalian target of rapamycin, Cancer Res. 69 (15) (2009) 6232–6240.
[20] B. Nyfeler, P. Bergman, E. Triantafellow, C.J. Wilson, Y. Zhu, B. Radetich, P.M. Finan, D.J. Klionsky, L.O. Murphy, Relieving autophagy and 4EBP1 from rapamycin resistance, Mol. Cell. Biol. 31 (14) (2011) 2867–2876.
[21] M.J. Deetz, C.C. Forbes, M. Jonas, J.P. Malerich, B.D. Smith, O. Wiest, Unusually low barrier to carbamate C-N rotation, J. Org. Chem. 67 (11) (2002) 3949–3952.
[22] B.D. Smith, D.M. Goodenough-Lashua, C.J.E. D'Souza, K.J. Norton, L.M. Schmidt, J.C. Tung, Substituent effects on the barrier to carbamate C-N rotation, Tetrahedron Lett. 45 (13) (2004) 2747–2749.
[23] Wu Ming-Yue, S.-F.W. Cui-Zan Cai, Jie-Qiong Tan, Min Li, Lu Jin-Jian, Xiu-Ping Chen, Yi-Tao Wang, Wei Zheng, Lu Jia-Hong, Natural autophagy blockers, dauricine (DAC) and daurisoline (DAS), sensitize cancer cells to camptothecin-induced toxicity, Oncotarget (2017) e20767.
[24] K.N. Dalby, I. Tekedereli, G. Lopez-Berestein, B. Ozpolat, Targeting the prodeath and prosurvival functions of autophagy as novel therapeutic strategies in cancer, Autophagy 6 (3) (2010) 322–329.
[25] S. Turcotte, A.J. Giaccia, Targeting cancer cells through autophagy for anticancer therapy, Curr. Opin. Cell Biol. 22 (2) (2010) 246–251.
[26] A. Kuma, M. Matsui, N. Mizushima, LC3, an autophagosome marker, can be incorporated into protein aggregates independent of autophagy, Autophagy 3 (4) (2007) 323–328.

[27] I. Tanida, T. Ueno, E. Kominami, LC3 and Autophagy, in: V. Deretic (Ed.), Autophagosome and Phagosome, Humana Press, Totowa, NJ, 2008, pp. 77–88.
[28] D.J. Klionsky, et al., Guidelines for the use and interpretation of assays for monitoring autophagy, Autophagy 12 (1) (2016) 1–222 (Third edition).
[29] V.K. Wong, T. Li, B.Y. Law, E.D. Ma, N.C. Yip, F. Michelangeli, C.K. Law, M.M. Zhang, K.Y. Lam, P.L. Chan, L. Liu, Saikosaponin-d, a novel SERCA inhibitor, induces autophagic cell death in apoptosis-defective cells, Cell Death Dis. 4 (2013) e720.
[30] J.A. Arnott, S.L. Planey, The influence of lipophilicity in drug discovery and design, Expert Opin Drug Discov 7 (10) (2012) 863–875.
[31] V.K. Wong, H. Zhou, S.S. Cheung, T. Li, L. Liu, Mechanistic study of saikosaponin-d (Ssd) on suppression of murine T lymphocyte activation, J. Cell. Biochem. 107 (2) (2009) 303–315.